# NATIONAL ADVISORY COMMITTEE FOR AERONAUTICS

REPORT No. 857

# ANALYSIS OF SPARK-IGNITION ENGINE KNOCK AS SEEN IN PHOTOGRAPHS TAKEN AT 200,000 FRAMES PER SECOND

By CEARCY D. MILLER, H. LOWELL OLSEN, WALTER O. LOGAN, Jr.
and GORDON E. OSTERSTROM

1946

For sale by the Superintendent of Documents, U. S. Government Printing Office, Washington 25, D. C. - - - - - - - - - - Price 15 cents

# AERONAUTIC SYMBOLS

## 1. FUNDAMENTAL AND DERIVED UNITS

| | Symbol | Metric | | English | |
|---|---|---|---|---|---|
| | | Unit | Abbreviation | Unit | Abbreviation |
| Length | $l$ | meter | m | foot (or mile) | ft (or mi) |
| Time | $t$ | second | s | second (or hour) | sec (or hr) |
| Force | $F$ | weight of 1 kilogram | kg | weight of 1 pound | lb |
| Power | $P$ | horsepower (metric) | | horsepower | hp |
| Speed | $V$ | kilometers per hour | kph | miles per hour | mph |
| | | meters per second | mps | feet per second | fps |

## 2. GENERAL SYMBOLS

$W$ Weight$=mg$

$g$ Standard acceleration of gravity$=9.80665$ m/s$^2$ or 32.1740 ft/sec$^2$

$m$ Mass$=\frac{W}{g}$

$I$ Moment of inertia$=mk^2$. (Indicate axis of radius of gyration $k$ by proper subscript.)

$\mu$ Coefficient of viscosity

$\nu$ Kinematic viscosity

$\rho$ Density (mass per unit volume)

Standard density of dry air, 0.12497 kg-m$^{-4}$-s$^2$ at 15° C and 760 mm; or 0.002378 lb-ft$^{-4}$ sec$^2$

Specific weight of "standard" air, 1.2255 kg/m$^3$ or 0.07651 lb/cu ft

## 3. AERODYNAMIC SYMBOLS

$S$ Area

$S_w$ Area of wing

$G$ Gap

$b$ Span

$c$ Chord

$A$ Aspect ratio, $\frac{b^2}{S}$

$V$ True air speed

$q$ Dynamic pressure, $\frac{1}{2}\rho V^2$

$L$ Lift, absolute coefficient $C_L=\frac{L}{qS}$

$D$ Drag, absolute coefficient $C_D=\frac{D}{qS}$

$D_0$ Profile drag, absolute coefficient $C_{D_0}=\frac{D_0}{qS}$

$D_i$ Induced drag, absolute coefficient $C_{D_i}=\frac{D_i}{qS}$

$D_p$ Parasite drag, absolute coefficient $C_{D_p}=\frac{D_p}{qS}$

$C$ Cross-wind force, absolute coefficient $C_C=\frac{C}{qS}$

$i_w$ Angle of setting of wings (relative to thrust line)

$i_t$ Angle of stabilizer setting (relative to thrust line)

$Q$ Resultant moment

$\Omega$ Resultant angular velocity

$R$ Reynolds number, $\rho\frac{Vl}{\mu}$ where $l$ is a linear dimension (e.g., for an airfoil of 1.0 ft chord, 100 mph, standard pressure at 15° C, the corresponding Reynolds number is 935,400; or for an airfoil of 1.0 m chord, 100 mps, the corresponding Reynolds number is 6,865,000)

$\alpha$ Angle of attack

$\epsilon$ Angle of downwash

$\alpha_o$ Angle of attack, infinite aspect ratio

$\alpha_i$ Angle of attack, induced

$\alpha_a$ Angle of attack, absolute (measured from zero-lift position)

$\gamma$ Flight-path angle

# REPORT No. 857

## ANALYSIS OF SPARK-IGNITION ENGINE KNOCK AS SEEN IN PHOTOGRAPHS TAKEN AT 200,000 FRAMES PER SECOND

By CEARCY D. MILLER, H. LOWELL OLSEN, WALTER O. LOGAN, Jr. and GORDON E. OSTERSTROM

Aircraft Engine Research Laboratory
Cleveland, Ohio

# National Advisory Committee for Aeronautics

*Headquarters, 1500 New Hampshire Avenue NW, Washington 25, D. C.*

Created by act of Congress approved March 3, 1915, for the supervision and direction of the scientific study of the problems of flight (U. S. Code, title 49, sec. 241). Its membership was increased to 15 by act approved March 2, 1929. The members are appointed by the President, and serve as such without compensation.


JEROME C. HUNSAKER, Sc. D., Cambridge, Mass., *Chairman*

THEODORE P. WRIGHT, Sc. D., Administrator of Civil Aeronautics, Department of Commerce, *Vice Chairman.*

Hon. WILLIAM A. M. BURDEN, Assistant Secretary of Commerce.

VANNEVAR BUSH, Sc. D., Chairman, Joint Research and Development Board.

EDWARD U. CONDON, PH. D., Director, National Bureau of Standards.

R. M. HAZEN, B. S., Chief Engineer, Allison Division, General Motors Corp.

WILLIAM LITTLEWOOD, M. E., Vice President, Engineering, American Airlines System.

EDWARD M. POWERS, Major General, United States Army, Assistant Chief of Air Staff–4, Army Air Forces, War Department.

ARTHUR W. RADFORD, Vice Admiral, United States Navy, Deputy Chief of Naval Operations (Air), Navy Department.

ARTHUR E. RAYMOND, M. S., Vice President, Engineering, Douglas Aircraft Co.

FRANCIS W. REICHELDERFER, Sc. D., Chief, United States Weather Bureau.

LESLIE C. STEVENS, Rear Admiral, United States Navy, Bureau of Aeronautics, Navy Department.

CARL SPAATZ, General, United States Army, Commanding General, Army Air Forces, War Department.

ALEXANDER WETMORE, Sc. D., Secretary, Smithsonian Institution.

ORVILLE WRIGHT, Sc. D., Dayton, Ohio.

---

GEORGE W. LEWIS, Sc. D., *Director of Aeronautical Research*

JOHN F. VICTORY, LLM., Executive Secretary

HENRY J. E. REID, Sc. D., Engineer-in-charge, Langley Memorial Aeronautical Laboratory, Langley Field, Va.

SMITH J. DEFRANCE, B. S., Engineer-in-charge, Ames Aeronautical Laboratory, Moffett Field, Calif.

EDWARD R. SHARP, LL. B., Manager, Aircraft Engine Research Laboratory, Cleveland Airport, Cleveland, Ohio

CARLTON KEMPER, B. S., Executive Engineer, Aircraft Engine Research Laboratory, Cleveland Airport, Cleveland, Ohio


---

## TECHNICAL COMMITTEES

AERODYANMICS
POWER PLANTS FOR AIRCRAFT
AIRCRAFT CONSTRUCTION
OPERATING PROBLEMS
MATERIALS RESEARCH COORDINATION
SELF-PROPELLED GUIDED MISSILES
SURPLUS AIRCRAFT RESEARCH
INDUSTRY CONSULTING COMMITTEE

*Coordination of Research Needs of Military and Civil Aviation*
*Preparation of Research Programs*
*Allocation of Problems*
*Prevention of Duplication*
*Consideration of Inventions*

---

LANGLEY MEMORIAL AERONAUTICAL LABORATORY, Langley Field, Va.

AMES AERONAUTICAL LABORATORY, Moffett Field, Calif.

AIRCRAFT ENGINE RESEARCH LABORATORY, Cleveland Airport, Cleveland, Ohio

*Conduct, under unified control, for all agencies, of scientific research on the fundamental problems of flight*

---

OFFICE OF AERONAUTICAL INTELLIGENCE, Washington, D. C.

*Collection, classification, compilation, and dissemination of scientific and technical information on aeronautics*

# REPORT No. 857

## ANALYSIS OF SPARK-IGNITION ENGINE KNOCK AS SEEN IN PHOTOGRAPHS TAKEN AT 200,000 FRAMES PER SECOND

By Cearcy D. Miller, H. Lowell Olsen, Walter O. Logan, Jr., and Gordon E. Osterstrom


### SUMMARY

*A motion picture of the development of knock in a spark-ignition engine is presented, which consists of 20 photographs taken at intervals of 5 microseconds, or at a rate of 200,000 photographs per second, with an equivalent wide-open exposure time of 6.4 microseconds for each photograph. A motion picture of a complete combustion process, including the development of knock, taken at the rate of 40,000 photographs per second is also presented to assist the reader in orienting the photographs of the knock development taken at 200,000 frames per second. The photographs taken at 200,000 frames per second are analyzed and the conclusion is made that the type of knock in the spark-ignition engine involving violent gas vibration originates as a self-propagating disturbance starting at a point in the burning or autoigniting gases and spreading out from that point through the incompletely burned gases at a rate as high as 6800 feet per second, or about twice the speed of sound in the burned gases. Apparent formation of free carbon particles in both the burning and the burned gas is observed within 10 microseconds after passage of the knock disturbance through the gases.*


### INTRODUCTION

Photography has been used in the study of combustion over a period of approximately 60 years beginning with the streak photographs taken by Mallard and Le Chatelier in 1883 (reference 1). Many investigators have used the photographic method for studying combustion in bombs and tubes of various types. (See reference 2 for specific mention of some of the investigations.) Streak photographs of combustion and knock in engine cylinders have been taken by Withrow and coworkers (references 3 to 7), by the Russian investigators Sokolik and Voinov (reference 8), and by Rothrock and Spencer (reference 9). The first actual motion pictures of knock combustion in an engine cylinder were presented by Withrow and coworkers during the period 1936 to 1940 (references 10 to 13).

Photographs of nonknocking combustion cycles also presented in references 10 to 13 were taken at speeds up to 5000 photographs (or frames) per second, whereas the photographs of knocking combustion cycles were taken at 2250 frames per second. Motion pictures of knocking and nonknocking combustion cycles taken at about 2000 frames per second were also presented by Rothrock and Spencer in 1938 (reference 9). The motion pictures taken at speeds of the order of 2000 frames per second were fast enough to show autoignition, or compression ignition, of the last part of the fuel-air charge to burn but were not fast enough to show all details of the knocking phenomenon. For that reason, early in 1936, the NACA undertook the development of a camera to take photographs of knocking combustion at the rate of 40,000 frames per second. The resulting high-speed camera is described in reference 14. Motion pictures of knocking combustion taken with this camera are presented in references 2 and 15 to 19.

Although autoignition of the last part of the charge to burn is often associated with knock, the pictures taken at 40,000 frames per second indicated that some phenomenon other than autoignition is responsible for the vibration of the combustion-chamber contents that gives rise to the ping associated with knock. This phenomenon that sets up the gas vibrations in the combustion chamber occurs within a time interval of not more than 50 microseconds (references 16 and 18). The camera operating at 40,000 frames per second takes only two photographs during an interval of 50 microseconds. This camera has a very pronounced focal-plane-shutter effect (reference 14), which badly distorts the records of movements taking place within a time interval as short as 50 microseconds. In reference 2 some of the pictures were analyzed by a method that takes the focal-plane-shutter effect into account and, in spite of the inadequate picture-taking rate, it was shown that the knocking phenomenon is a self-propagating disturbance whose speed varies in different cases from about the speed of sound in the combustion chamber to about twice the speed of sound. Sokolik and Voinov (reference 8) had previously concluded from their streak photographs that the knocking phenomenon is a detonation wave traveling at about twice the speed of sound in the combustion chamber.

Because the high-speed camera was not fast enough to produce a clear picture of the development of knock, work was started in 1939 at the NACA Langley Field laboratory on the development of a still faster camera. This work resulted, early in 1939, in the invention of a new optical system entirely unlike the optical system of the high-speed camera

described in reference 14. The camera that has been constructed according to the new optical principle will be designated hereinafter the ultra-high-speed camera in contradistinction to the older 40,000-frame-per-second camera which, as in the past, will be designated the high-speed camera. Credit should be given to Alois Krsek, Jr., and Newell D. Sanders of the NACA technical staff for valuable suggestions in the design of the ultra-high-speed camera.

The ultra-high-speed camera was constructed at the NACA Ames laboratory in 1941. Attempts were made to operate the camera at the Langley Field laboratory in 1942 and at the Cleveland laboratory from 1943 to the present time. A number of serious difficulties were encountered in the operation of the camera and its operation is not yet regarded as entirely satisfactory. One motion picture of the knocking phenomenon has been obtained, however, at the rate of 200,000 frames per second. The present paper presents and analyzes this single motion picture.

## APPARATUS AND PROCEDURE

**Combustion apparatus.**—The single knocking combustion cycle that is the subject of this report occurred in the same combustion apparatus that was used in the experiments presented in references 2, 9, and 15 to 19. A diagrammatic sketch of this apparatus is given in figure 1; the apparatus has been described in references 9 and 16.

As in previous investigations, the combustion apparatus was driven at the test speed by an electric motor and was fired for only one cycle. During the one power cycle of the engine a single charge of fuel was injected on the intake stroke, a single spark was produced at the spark plug, and a series of photographs of the knocking phenomenon was taken.

**Engine operating conditions.**—The engine operating conditions for the combustion cycle studied were as follows:

| | |
|---|---|
| Engine coolant temperature, °F | 250 |
| Compression ratio | 7 |
| Engine speed, rpm | 500 |
| Fuel-air ratio (approximate) | 0.08 |
| Spark timing, deg B. T. C. | 27 |

Only one spark plug was used, in position G in the cylinder head. (See fig. 1.) The fuel used was a blend of 70 percent S–3 reference fuel with 30 percent M–2 reference fuel.

**Setup for schlieren photography.**—The optical setup for schlieren photography was somewhat different from that used for the work of references 2 and 15 to 19 but produced practically the same results. In the earlier work a fairly sensitive schlieren system was used. The mirror on the piston top (fig. 1) forms a part of the optical system and, inasmuch as it is impossible to constrain this mirror from shifting its angular position because of piston slap, considerable difficulty has been encountered with the sensitive schlieren system. For that reason and because the sensitive

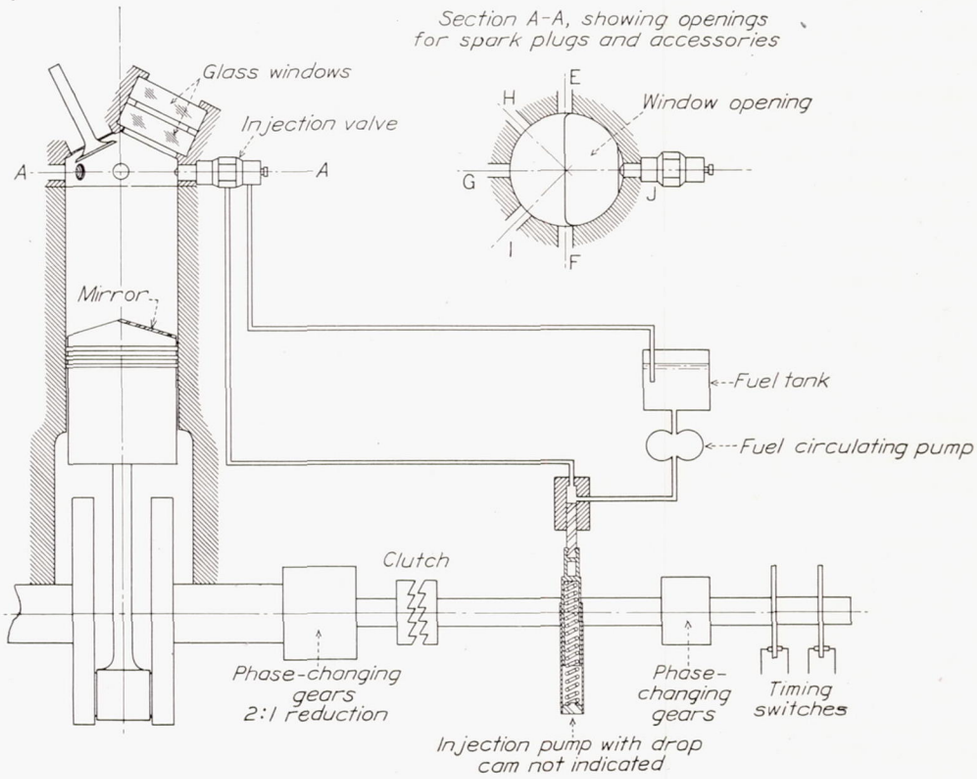


FIGURE 1.—Diagrammatic sketch of combustion apparatus.

schlieren system recently had been found unnecessary in work with the high-speed camera, the optical setup was modified to the form shown in figure 2. In this form of the optical setup, light from the source (a gas-filled flash tube for the ultra-high-speed photographs presented herein) passes through the schlieren lens from right to left and is brought into approximate parallelism by this lens. The light then is reflected from the external mirror through the glass windows in the cylinder head to the top of the piston. The mirror on the piston top returns the light to the external mirror from which it passes back through the schlieren lens from left to right. As the light passes through the schlieren lens from left to right it is refracted by this lens so as to form an image of the light source on the camera lens. The camera lens refracts the light in such a manner as to produce an image of the combustion-chamber contents on the film in the camera.

In any part of the combustion chamber in which combustion is not taking place, the light passes through practically unaffected. Such parts of the combustion chamber, as photographed by the camera, consequently appear as white regions on the positive prints. In any part of the combustion chamber where burning is taking place, however, the light rays seem to be thoroughly scattered; the schlieren lens is therefore not able to focus the light rays on the camera lens after they have passed through the combustion zones. The combustion zones, for this reason, show up on the positive prints as black regions. (All photographs reproduced in this paper are positive prints.)

**Ultra-high-speed camera.**—The ultra-high-speed camera does not have a focal-plane shutter as does the high-speed camera described in reference 14. The optical characteristics of the shutter of the ultra-high-speed camera are the same as those of a conventional between-the-lens shutter. The distortion of high-speed phenomena, which caused the difficulty in interpreting photographs taken with the high-speed camera, is therefore absent. There is some overlapping of exposures, as shown in figure 3. This figure shows

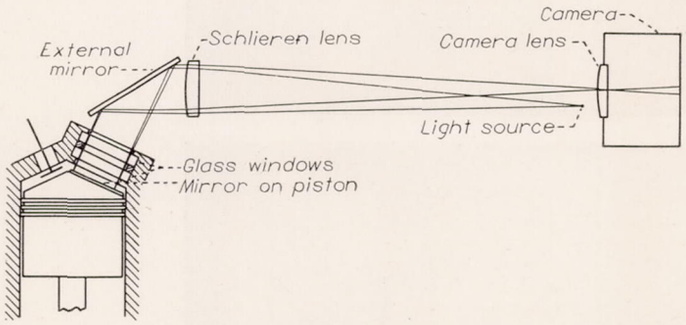


FIGURE 2.—Diagrammatic sketch of optical system for taking schlieren photographs of knock at 200,000 frames per second.

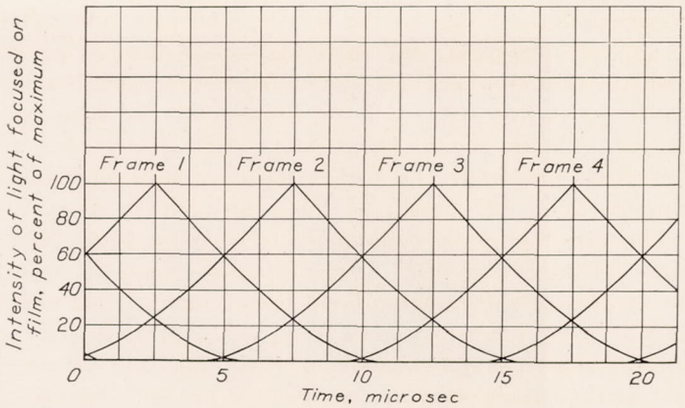


FIGURE 3.—Variation with time of intensity of light focused on film by ultra-high-speed camera for several motion-picture frames.

the variation with time of the intensity of the light focused on the film for each of several successive frames. The curves of figure 3 are directly applicable when the camera is operated at 200,000 frames per second; operation at any other speed would involve only a change of the time scale of the figure. As may be determined from the figure, about 60 percent of the integrated intensity-time product for any one frame occurs within the 5-microsecond interval allotted for that frame, whereas 20 percent of the integrated product falls within each of the 5-microsecond intervals allotted to the preceding and succeeding frames. The equivalent wide-open time of the shutter is 6.4 microseconds with operation at 200,000 frames per second.

## PRESENTATION OF PHOTOGRAPHS

### GENERAL VIEW OF PHOTOGRAPHS

Figure 4 shows the pictures of the knocking phenomenon taken at 200,000 frames per second as a series of 20 still pictures. The photographs were taken in the order from left to right across the top row, then from left to right across the second row, and so on. Hereinafter individual frames in the series will be designated frame A–1, meaning the first frame of the first row, frame B–3, meaning the third frame of the second row, and so on.

The 20 frames of figure 4 represent only a small fraction of the total combustion process. For this reason figure 5 has been provided to assist the reader in the orientation of figure 4. Figure 5 is the same shot of knocking combustion taken at 40,000 frames per second that was published as figure 10 in reference 2 and as figure 11 in reference 19. Figure 5 is not a photograph of the same combustion cycle as that of figure 4 but is a photograph of a somewhat similar cycle. The combustion cycle shown in figure 5 differs from that of figure 4 in the fact that two spark plugs were fired, one at position F and the other at position G (see fig. 1), whereas

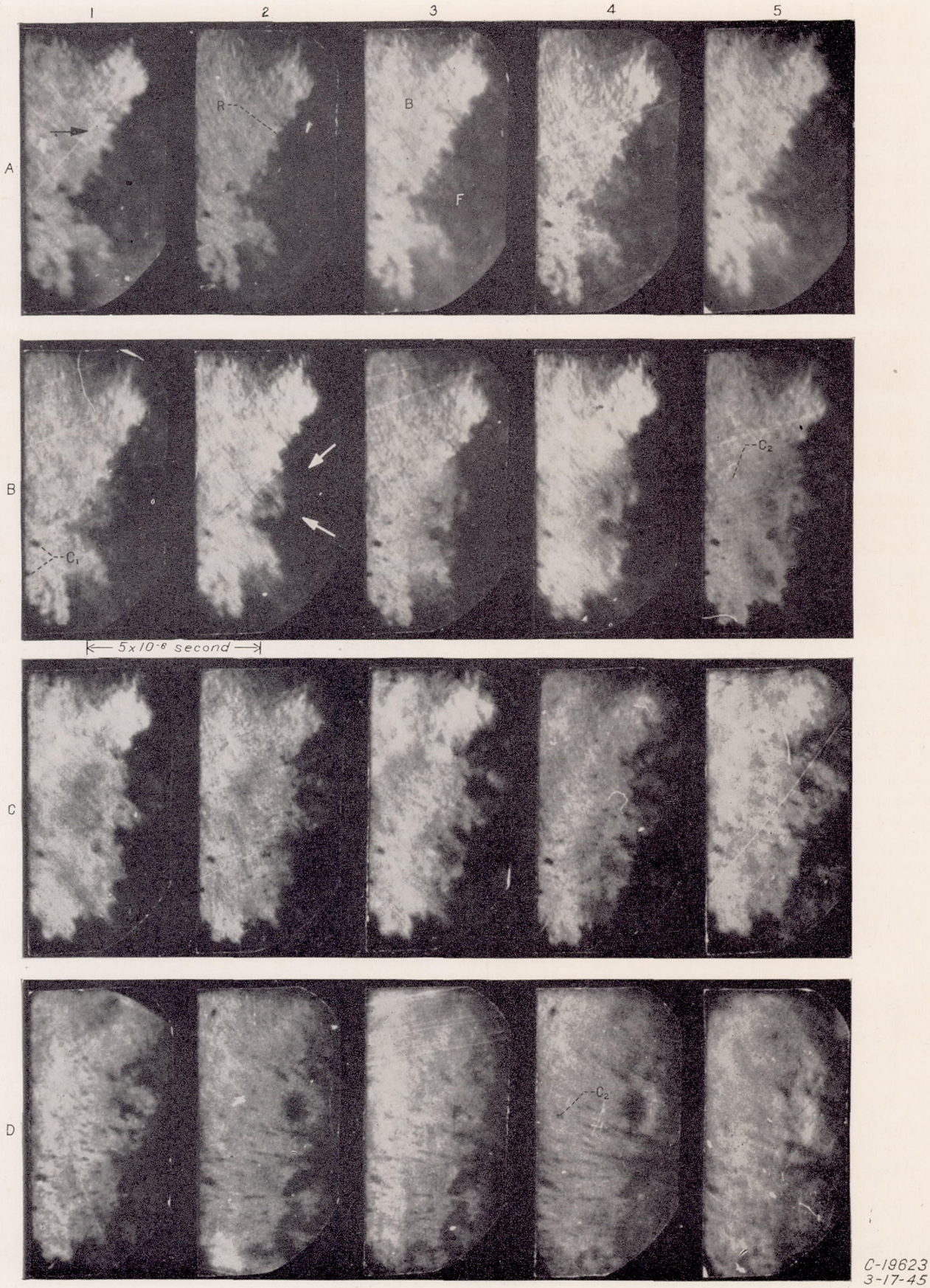


FIGURE 4.—Knocking phenomenon photographed at 200,000 frames per second with ultra-high-speed camera

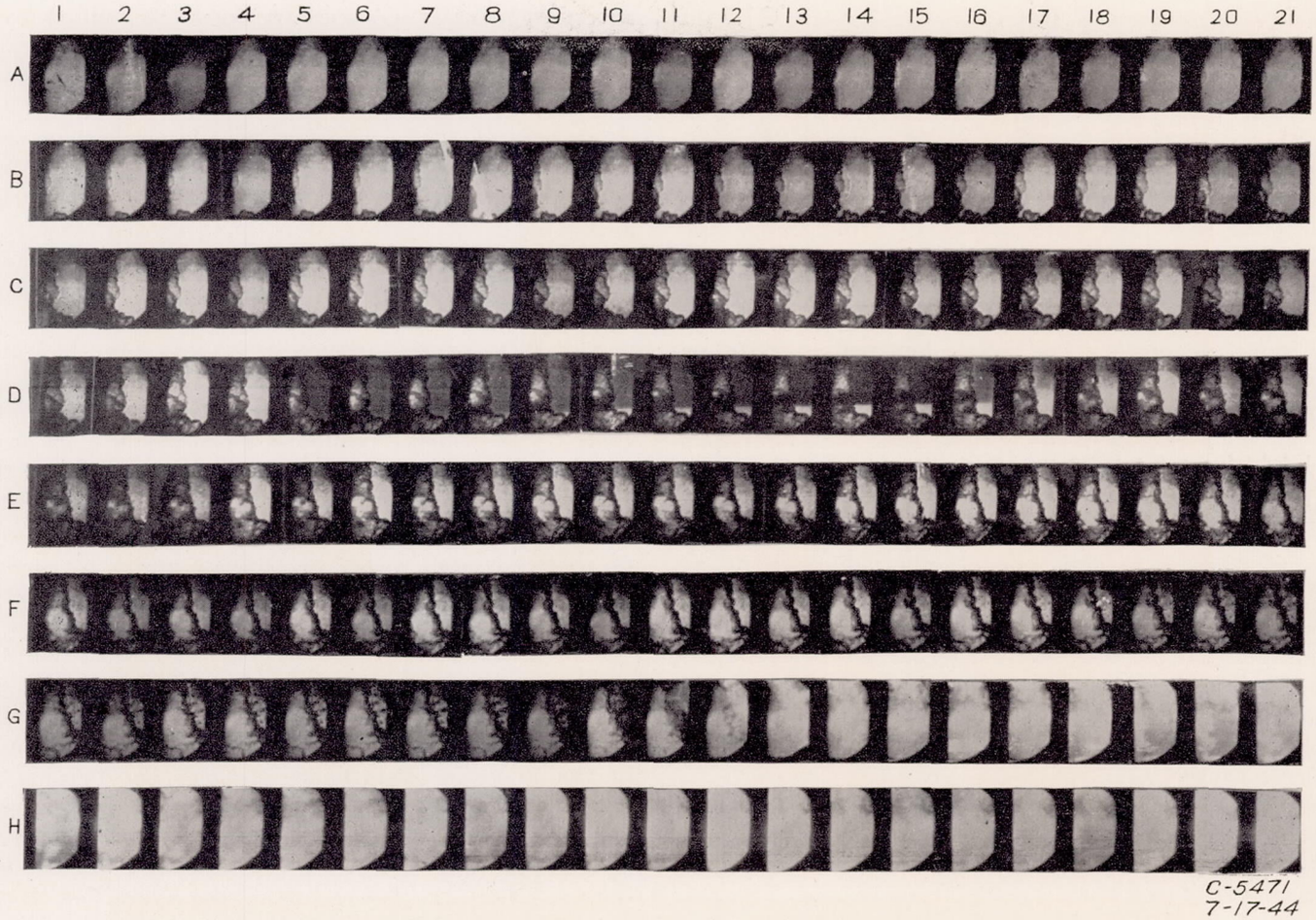


FIGURE 5.—Knocking combustion cycle photographed at 40,000 frames per second. (See references 2 and 19, figs. 10 and 11, respectively.)

only the spark plug in G position was used for the combustion process shown in figure 4. In figure 5, the flame from the spark plug in F position first comes into view between frames A–4 and A–10. The flame from the spark plug in G position becomes clearly visible in the first few frames of row B and is faintly visible in the later frames of row A. In the frames of rows A through C the two flames merge and progress well into the field of view. Up to about the end of row C the flame appears as a solid dark cloud. In frames D–5 to D–16 of the figure a dark streak appears, which is due to faulty processing of the film and should be ignored. In frames D–17 to D–21 and the frames of row E the flame no longer appears as a solid dark cloud; instead a white spot develops within the flame and gradually grows larger. By the time the conditions of frame F–13 are reached this white spot has grown till it includes most of the flame. This white region within the flame probably represents the portion of the flame in which normal combustion is complete, whereas the dark regions represent the portions of the flame in which combustion is in progress. In frame F–13 the dark cloud extending from the upper central part of the frame downward to the lower right portion of the frame probably represents burning gases as does the dark cloud in the lower left corner of the frame. This fact has been indicated by the work of references 18 and 20. The white region to the right of the dark cloud in frame F–13, of course, represents gases that have not yet been ignited, or what is commonly referred to as the "end gas." In the frames from F–13 to F–21 autoignition begins in the end gas as shown by the black dots that develop in the end gas in these frames. In frames G–1 to G–10 these black spots of autoignition gradually become larger until, in frame G–10, they fill the entire end zone. In frames G–11 and G–12 knock occurs. In reference 2 the knock that appears in frames G–11 and G–12 was shown to be a progressive disturbance traveling at a speed of the order of the speed of sound in the burned gases.

With reference again to the ultra-high-speed photographs of figure 4, the five frames shown in row A of this figure were taken at about the same stage of the combustion process as frame G–10 of figure 5. The entire series of 20 frames shown in figure 4 covers the same stages in the combustion

and knocking process as frames G–10 through G–13 of figure 5; the dark combustion zone disintegrates in the 20 frames of figure 4 and also in frames G–10 through G–13 of figure 5. Whereas in frame G–10 of figure 5 the autoignited end zone appears as a dark cloud covering the right and upper portions of the frame, in the frames of row A of figure 4 the burning end zone appears as a dark cloud covering the right and lower portions of the frame (the region marked F in frame A–3 of fig. 4). The region designated B in frame A–3 of figure 4 represents the gases in which combustion has been completed before the exposure of the frames of row A. The line of demarcation R (frame A–2), between the white or gray portions of these frames and the dark burning portions, represents not the front of the flame but the rear edge of the burning zone. The direction of flame travel is indicated by the arrow in frame A–1 of the figure.

Photographs were not taken far enough in advance of the frames of figure 4 to determine whether autoignition occurred. On the basis of observation of several hundred previous shots taken at 40,000 frames per second, however, it is believed that the dark region designated F in the frames of row A of figure 4 does represent burning gases, whether these gases were ignited by the flame front or by autoignition, and that this dark region is not due to some unforeseen extraneous cause.

Careful comparison of frames A–1 through B–1 in figure 4 will reveal no very marked difference between any two successive frames except as to the quality of the definition. Frames A–1, A–3, and A–5 are rather badly blurred. Frames A–2, A–4, and B–1 are much more sharply defined. This alternate blurring and sharpening in these frames is a characteristic introduced by the camera, which it is believed can be eliminated as further work is done with the camera. In contrast to the negligible change that occurs between any two successive frames from frame A–1 to B–1, a marked change occurs between frames B–1 and B–2, between frames B–2 and B–3, and between frames B–3 and B–4. The change between frames B–1 and B–2 consists in the development of a very appreciable whitened region in the combustion zone as seen in frame B–2. This whitened region was very much less apparent in frame B–1 and in each of the frames of row A. Two white arrows have been drawn on frame B–2, each arrow pointing at the center of the whitened region referred to. The continued disintegration of the dark combustion zone in frames B–3 and B–4, as compared with frame B–2, is very plain. Because of the extreme rapidity of the changes occurring between the exposures of successive frames in row B of figure 4, it is believed that the phenomenon of knock began during the exposures of these frames.

A startling conclusion appears evident from the frames of row B of figure 4; namely, that at least in this case the knocking phenomenon started at the rear edge of the combustion zone. This evidence reinforces a conclusion made in reference 18 from a study of the photographs taken at 40,000 frames per second to the effect that knock apparently originates only in a part of the fuel-air charge that has been previously ignited, either by autoignition or by passage of the flame front, but which has not burned to completion.

### APPARENT SPEED OF KNOCKING DISTURBANCE THROUGH BURNING GASES

In figure 6 the five frames of row B from figure 4 have been reproduced and used to determine the apparent speed of the knocking disturbance through the burning gases. The line of demarcation $R_{B-1}$ between the burning gas and the burned gas has been accentuated by a black line drawn in the first frame of figure 6. This same demarcation line, obtained from the first frame of the figure, has also been drawn on each of the other frames of the figure. All whitening or graying of the combustion zone to the right of the black line in any frame of the figure has been assumed to be caused by the knock reaction and the whitening or graying has further been assumed to indicate the full extent of the knocking disturbance in any frame of the figure. In each frame after the first, horizontal straight lines have been drawn marking the upper and lower limits of the whitening or graying, respectively, of the combustion zone. The dis-

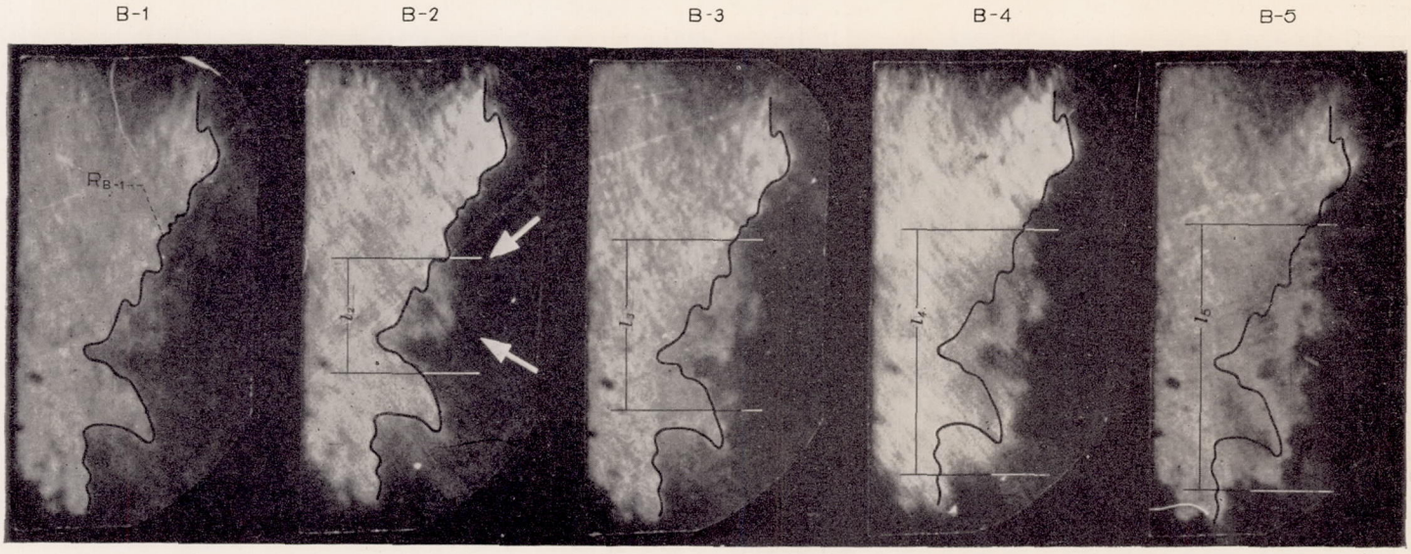


C-19623
10-1-47

FIGURE 6.—Effect of self-propagating knock reaction on burning gases during earliest stages of knock development.

tance between the two horizontal lines has been designated $l_2$, $l_3$, $l_4$, and $l_5$ in frames 2, 3, 4, and 5, respectively, of the figure. The value of $l_1$ has been assumed equal to zero in the first frame of the figure. The difference between the values of $l$ in any two successive frames may be considered to represent the combined upward and downward travel of the knocking disturbance that occured in the time interval between the exposures of the two successive frames. The following velocities $V$ have been determined for the knocking disturbance according to the equation

$$V=\frac{1}{2}\left(\frac{l_2-l_1}{5\times10^{-6}}\right)$$

| Frames: | *Velocity of knocking disturbance, (ft/sec)* |
|---|---|
| 1–2 | 9200 |
| 2–3 | 4200 |
| 3–4 | 6900 |
| 4–5 | 1200 |

The average of the first three velocities determined is nearly 6800 feet per second. This value checks very well with the speed of about 2000 meters per second determined by Sokolik and Voinov (reference 8) and with the highest speeds determined in reference 2. This speed is fully as great as should be expected for a true detonation wave.

The fourth velocity determined, between frames 4 and 5 of figure 6, is comparatively very low. Moreover, comparison of the frames of rows C and D of figure 4 with frame B–5 of that figure reveals no evidence of a progressive disturbance such as is apparent in frames B–2, B–3, and B–4. The dark combustion zone does gradually disintegrate in the frames of rows C and D of the figure. This disintegration of the dark combustion zone is many times more rapid than the disintegration that would occur with nonknocking combustion. (See references 16 to 18.) It is, however, much slower than the disintegration of portions of the combustion zone that is seen in frames B–2, B–3, and B–4 and it appears to be quite homogeneous throughout the combustion zone, not showing the progressive tendency in the spatial sense that is seen in frames B–2, B–3, and B–4.

It is not fully understood why a spatially progressive disturbance (presumably a detonation wave) causes complete disintegration of portions of the combustion zone but only causes a homogeneous speeding up of the combustion in the other parts of the combustion zone. It seems possible that those portions of the combustion zone that disintegrated in frames B–2, B–3, and B–4 may have been the only parts of the zone in a sufficiently advanced stage of combustion to be detonatable. When the detonation wave passed beyond the limits of the detonatable gases, it may have degenerated into an adiabatic shock wave. This shock wave may have had the effect of speeding up the combustion and perhaps in some way changing the nature of the combustion in the remaining incompletely burned gases. Another possible explanation of this phenomenon is presented under CARBON FORMATION.

### EFFECT OF KNOCKING DISTURBANCE ON BURNED GASES

When the photographs taken at 200,000 frames per second are projected on the screen as motion pictures, two very high-speed waves are visible traveling one after the other out through the burned gases away from the center of the knocking disturbance just after knock occurs. The first of the two waves through the burned gas after the occurrence of knock is indicated in figure 7, which, like figure 6, is a reproduction of frames B–1 to B–5 of figure 4. In figure 7, however, dashed black lines have been drawn in frames 2, 3, and 4 outlining blurred regions that appear in the burned gas. The definition of the photographs is not sufficiently good that the blurred regions can be outlined with absolute certainty. The authors, however, have had the advantage of observation of the photographs again and again as motion pictures projected on a screen and they

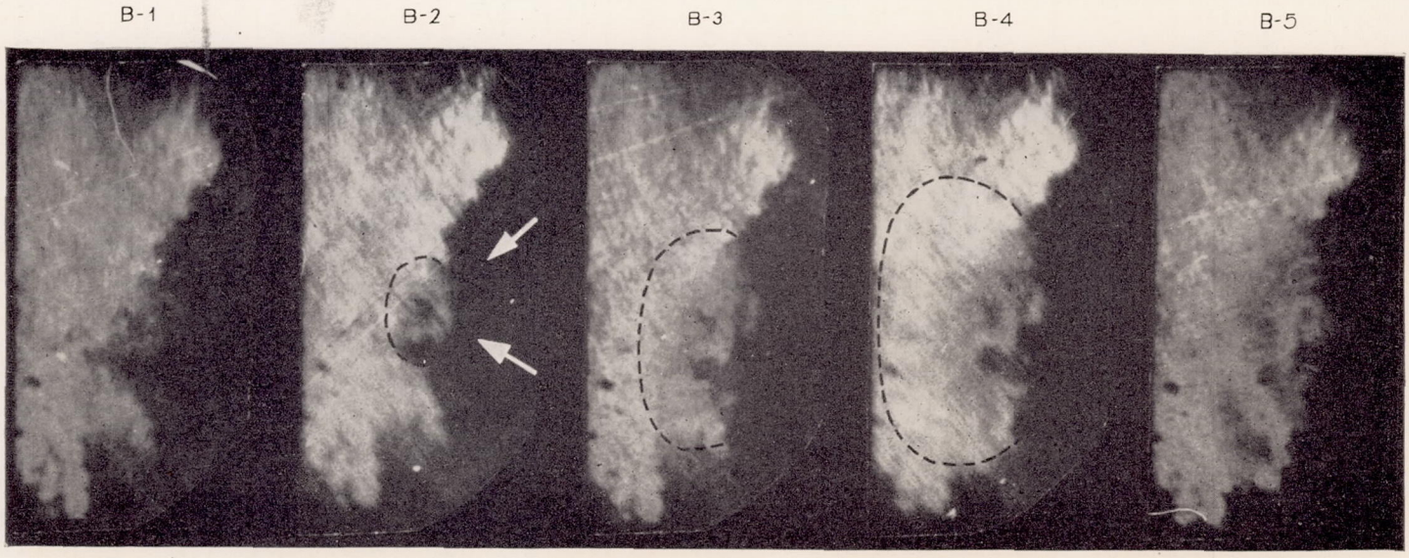


C-19623
10-1 47

FIGURE 7.—Apparent propagation of primary wave through burned gases during earliest stages of knock development

also have the advantage of direct observation of the original photographs, which are inevitably of better quality than the printed reproductions. It is believed that the dashed outlines shown in figure 7 represent the first wave seen traveling out through the burned gas in the projected motion pictures with an inaccuracy not greater than a small percentage of the wave travel between successive frames.

The leftward extremity of the dashed outline in frame 3 of figure 7 is considerably farther to the left than in frame 2. Likewise the leftward extremity of the dashed outline in frame 4 is considerably farther to the left than in frame 3. The leftward travel of the extremity of the outline between frames 2 and 3 and between frames 3 and 4 appears to have been at a velocity of about 6500 feet per second. This value checks well with the average speed determined in the burning gas from figure 6.

The second of the two waves that travel out through the burned gas after the start of knock is indicated in figure 8. The frames of figure 8 are frames B–5 to C–4 of figure 4. Darkened and blurred regions in the burned gases are outlined in figure 8 with dashed black lines. Between frames 1 and 2 (order number refers to arrangement in fig. 8, not arrangement in row C of fig. 4) and between frames 2 and 3 the leftward extremities of the dashed outlines traveled toward the left with velocities of about 5800 and 5400 feet per second, respectively. Between frames 3 and 4 and between frames 4 and 5, the rightward extremities of the dashed outlines traveled to the left with a velocity of about 7000 feet per second (not very definite between frames 3 and 4 but apparently at least 7000 ft/sec in this case). The average of the four determinations for the second wave through the burned gas is about 6300 feet per second, less than the average of 6500 feet per second for the first wave by an amount not greater than the probable error of the determinations.

Evidence of two successive waves, traveling through the burned gas, each at a velocity about twice the speed of sound, is confusing. It is difficult to believe that any explosive chemical reaction could occur in the burned gas that would release enough energy to support a violent detonation wave. It is still more difficult to believe that two explosive chemical reactions could occur in the burned gas, one after the other, each releasing enough energy to support a violent detonation wave. According to hydrodynamic theory (references 21 and 22), a stable detonation wave traveling through the burned gas at 6300 feet per second would require an energy release roughly equal to the entire heating value of the fuel.

Waves of transverse deflection of the mirror on the piston top are a possible explanation of the two apparent waves traveling through the burned gases. Such waves in mirrors following knock have actually been observed in photographs taken at 40,000 frames per second but not yet published. When the photographs of figure 4 are projected on the motion-picture screen, the visual impression is that the waves through the burned gases are actually gas waves. Until definite evidence is available, however, that these waves cannot be transverse waves in the glass, speculation about their significance as gas waves will probably not be very fruitful.

### CARBON FORMATION

Black spots, probably free carbon particles formed by the knock reaction, are clearly visible in frame B–5 and the frames of rows C and D of figure 4. Throughout this report these spots, and similar spots in other figures, will be referred to as "carbon particles" with the understanding that the identity of the spots as carbon particles has not been scientifically proved. It is the authors' feeling, from study of the figures of this report and numerous previous photographs taken at 40,000 frames per second, that carbon particles are by far the most likely explanation of the spots. Throughout the frames of row D of figure 4, the extreme right edge of the frame remains dark, possibly because of a heavy concentration of carbon particles near the chamber wall. Free

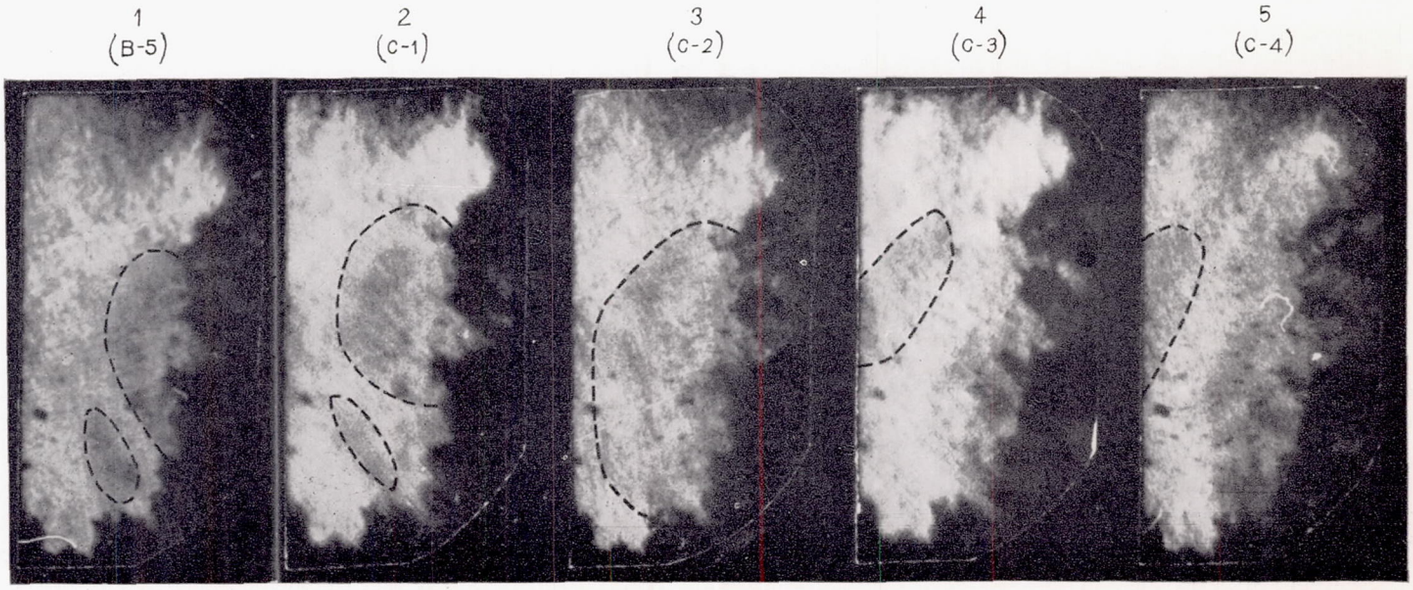


C-19623
10-1 47

FIGURE 8.—Apparent propagation of secondary wave through burned gases during later stages of knock development.

carbon particles have not generally been observed in the photographs taken at 40,000 frames per second, probably because the externally supplied light used in the taking of those photographs nearly matched the incandescence of the carbon particles. The carbon particles are visible, however, as brilliant white spots in a few of the photographs taken at 40,000 frames per second, notably figure 8 of reference 16 (same as fig. 6 of reference 2). It is clear from the figure of reference 16 and other unpublished photographs of knocking combustion taken at 40,000 frames per second, that free carbon is formed in the cylinder charge within 25 microseconds after the passage of the knock disturbance through the charge. For the photographs of figure 4, the exposure time and the lens aperture were so small that the incandescence of the carbon particles did not photograph. The externally supplied light was so brilliant that the carbon particles show up in the photographs as dark shadows.

A few carbon particles were formed in the combustion cycle of figure 4 well before the knock disturbance began, for example, the two particles designated $C_1$ in frame B–1. (Some carbon particles may be formed, of course, even with nonknocking combustion.) The number of carbon particles, however, increases manyfold in row C of figure 4 after passage of the knock disturbance through the charge. These particles show up as small black dots in the frames of row C and to some extent in frame B–5. In the frames of row D, however, each of the carbon particles smears out to form a line about 1/4 inch long (actual combustion-chamber scale) extending in the direction of the gas motion. (The incandescent spots of carbon seen in fig. 8 of reference 16 were in the form of slender streaks.) Apparently the carbon particles have sufficient inertia that they are temporarily left behind by the mass motion of the gases. The visible particles are probably feathery conglomerations of much smaller particles. As the gases move by the visible particles at high speed in the frames of row D, successive outer layers of the smaller particles may be sheared off and carried along with the moving gases with the final result that each visible particle is drawn out into a long slender streak. The carbon particles may also serve as nuclei for the precipitation of additional carbon from the gases flowing by. The precipitation of additional carbon during the formation of the streaks seems likely because the density of the streaks appears to be as great as the density of the original black dots and the width of the streaks appears as great as the diameters of the original black dots.

It is interesting to note that many of the carbon particles are formed in the gases that were burned before passage of the self-propagating knock reaction. Some of these spots are formed early enough in the process, and far enough from the burning zone, to preclude any possibility that they are actually formed in the burning gases and physically carried into the position of the burned gas. The particle designated $C_2$ in frame D–4 of figure 4, for example, is already visible in frame B–5 in the original photographs, though this spot may not reproduce well enough to be visible in the printed figure in frame B–5. This carbon particle was formed in frame B–5 not more than 20 microseconds after the beginning of the knock disturbance (frame B–1 or B–2) and not more than 10 microseconds after the passage of the knock disturbance through the location of the particle $C_2$ in frame B–3. (See fig. 7.)

### NATURE OF SELF-PROPAGATING KNOCK REACTION

The hydrodynamic theory of stable detonation waves requires a positive motion of the reacted gases immediately behind the detonation front in the direction of motion of the detonation wave and at a speed equal to the speed of the detonation wave minus the speed of sound in the burned gas. Throughout the entire course of the knock investigations made with the high-speed camera at 40,000 frames per second, which covered a period of over 5 years and included hundreds of motion pictures of knocking combustion, no evidence has ever been found of a mass motion of the gases caused directly by the passage of the knocking disturbance through the gases. Mass motion of the gases has always been evident in the form of a vibration of the gases, which is responsible for the knocking sound, but this vibration has always appeared to get under way after the knock disturbance passed completely through the charge. Any configurations visible before the occurrence of knock in either the burned gases or the burning gases, if they remained visible after the knock disturbance had passed through them, appeared entirely unmoved physically by the passage of the knock disturbance. The impression that the gases are not noticeably set in motion by the passage of the original knock reaction is unaltered in the ultra-high-speed pictures presented in the figures of this report.

Upon examination of the frames of figure 6, all configurations of the burning gases (to the right of the demarcation line $R_{B-1}$) that are visible in more than one frame of the figure will be seen to occupy the same position in one frame as in another, relative to the demarcation line. None of them show any evidence of having been moved physically by the passage of the detonation wave. Small carbon particles appear at various points throughout the field of view in the frames of rows B and C of figure 4. Although the detonation wave passed through the charge in the frames of row B, the carbon particles do not show evidence of motion until the frames of row D in which the mass motion of the gas finally gets under way and causes the particles to smear out into streaks. This mass motion of the gas, getting under way in the frames of row D, appears too late to have been caused directly by the spatially progressive disturbance seen in frames B–2, B–3, and B–4. The mass motion occurred immediately after the gradual disintegration of the dark combustion zone that is seen in frames B–5 to D–2. The motion was therefore probably caused by a local high pressure produced by the reaction responsible for this gradual disintegration of the dark combustion zone.

The photographs taken at 40,000 frames per second are too slow and those taken at 200,000 frames per second are too indistinct to allow a quite definite conclusion that the knocking detonation wave does not have the follow-through velocity that should be expected of a stable detonation wave. The authors do not feel, however, that the absence of the follow-through velocity would cast doubt upon the correctness of the conclusion that some kind of a detonation wave

actually does occur. The theoretical possibility of unstable detonation waves traveling at a speed higher than that of the stable detonation wave corresponding to the same energy release has been indicated by Becker (reference 21). He cited experiments by Kast (reference 23) in which such unstable detonation waves were produced with a number of explosives. Such unstable detonation waves should probably not be expected to show the same follow-through motion as the stable detonation wave. Water-condensation waves, apparently involving condensation of water but no chemical reaction, have been observed in the flow of humid air through supersonic nozzles by Hermann (reference 24) and in unpublished NACA records. These stationary waves apparently involve much less change of velocity of the air mass than do stable detonation waves in explosive gas mixtures. A self-propagating reaction might occur, moreover, in which the propagation is not caused by a shock wave but by the diffusion of chain carriers of low molecular weight. In such a case the average carrier would travel a distance equal to the mean free path and would bypass most of the gas molecules; the propagation rate would depend on the speed of the carriers rather than on the dynamics of a shock wave. Lewis (reference 25) has previously proposed the idea that propagation rates of detonation waves may be governed by the velocities of certain carriers involved in a chain reaction and has succeeded in naming suitable carriers for detonations of a number of substances. Cowling (reference 26) has presented a mathematical discussion of the effect of diffusion on the propagation of shock waves.

Until more definite evidence is available as to the existence of a follow-through velocity, the simplest and most logical interpretation of the photographs of this report and of reference 2 seems to be that the type of knock involving gas vibrations is caused by some type of detonation wave originating at random at some point within the burning or autoigniting gases and spreading out in all directions from the point of origin at a rate ranging from the speed of sound in the burned gases to twice the speed of sound in the burned gases.

## CONCLUSIONS

The present paper is based entirely on a single photographic shot of the knock phenomenon taken at the rate of 200,000 frames per second. All conclusions should therefore be regarded as tentative until it is possible to supplement the study with additional photographs. The conclusions may probably be regarded as definite for the single knocking cycle studied but they cannot, of course, be regarded as generally applicable to all knocking cycles. The tentative conclusions that seem justified by the appearance of the photographs are as follows:

1. The type of knock in the spark-ignition engine involving violent gas vibration originates as a self-propagating disturbance starting at a point in the burning or autoigniting gases and spreading out from that point through the incompletely burned gases at a rate as high as 6800 feet per second, or about twice the speed of sound in the burned gases.

2. Apparent free carbon particles are formed in both the burning and the burned gases within 10 microseconds after passage of the knock reaction through the gases.

Aircraft Engine Research Laboratory,
National Advisory Committee for Aeronautics,
Cleveland, Ohio, *April 10, 1946*.

## REFERENCES

1. Mallard, and Le Chatelier: Recherches Expérimentales et Théoriques sur la Combustion des Mélanges Gazeux Explosifs. Deuxième Mémoire sur la Vitesse de Propagation de la Flamme dans les Mélanges Gazeux. Annales des Mines, Sér. 8, t. IV, 1883, pp. 296–378.
2. Miller, Cearcy D.: Relation between Spark-Ignition Engine Knock, Detonation Waves, and Autoignition as Shown by High-Speed Photography. NACA Rep. No. 855, 1946.
3. Withrow, Lloyd, and Boyd, T. A.: Photographic Flame Studies in the Gasoline Engine. Ind. and Eng. Chem., vol. 23, no. 5, May 1931, pp. 539–547.
4. Withrow, Lloyd, and Rassweiler, Gerald M.: Spectroscopic Studies of Engine Combustion. Ind. and Eng. Chem., vol. 23, no. 7, July 1931, pp. 769–776.
5. Rassweiler, Gerald M., and Withrow, Lloyd: Emission Spectra of Engine Flames. Ind. and Eng. Chem., vol. 24, no. 5, May 1932, pp. 528–538.
6. Rassweiler, Gerald M., and Withrow, Lloyd: Spectrographic Detection of Formaldehyde in an Engine Prior to Knock. Ind. and Eng. Chem., vol. 25, no. 12, Dec. 1933, pp. 1359–1366.
7. Withrow, Lloyd, and Rassweiler, Gerald M.: Engine Knock. The Auto. Eng., vol. XXIV, no. 322, Aug. 1934, pp. 281–284.
8. Sokolik, A., and Voinov, A.: Knocking in an Internal-Combustion Engine. NACA TM No. 928, 1940.
9. Rothrock, A. M., and Spencer, R. C.: A Photographic Study of Combustion and Knock in a Spark-Ignition Engine. NACA Rep. No. 622, 1938.
10. Withrow, Lloyd, and Rassweiler, Gerald M.: Slow Motion Shows Knocking and Non-Knocking Explosions. SAE Jour., vol. 39, no. 2, Aug. 1936, pp. 297–303, 312.
11. Rassweiler, Gerald M., and Withrow, Lloyd: Motion Pictures of Engine Flames Correlated with Pressure Cards. SAE Jour., vol. 42, no. 5, May 1938, pp. 185–204.
12. Rassweiler, Gerald M., Withrow, Lloyd, and Cornelius, Walter: Engine Combustion and Pressure Development. SAE Jour. (Trans.), vol. 46, no. 1, Jan. 1940, pp. 25–48.
13. Withrow, Lloyd, and Cornelius, Walter: Effectiveness of the Burning Process in Non-Knocking Engine Explosions. SAE Jour. (Trans.), vol. 47, no. 6, Dec. 1940, pp. 526–545.
14. Miller, Cearcy D.: The NACA High-Speed Motion-Picture Camera. Optical Compensation at 40,000 Photographs per Second. NACA Rep. No. 856, 1946.
15. Rothrock, A. M., Miller, Cearcy D., and Spencer, R. C.: Slow Motion Study of Normal Combustion, Preignition, and Knock in a Spark-Ignition Engine. NACA Tech. Film No. 14, 1940.
16. Rothrock, A. M., Spencer, R. C., and Miller, Cearcy D.: A High-Speed Motion-Picture Study of Normal Combustion, Knock, and Preignition in a Spark-Ignition Engine. NACA Rep. No. 704, 1941.
17. Miller, Cearcy D.: A Study by High-Speed Photography of Combustion and Knock in a Spark-Ignition Engine. NACA Rep. No. 727, 1942.
18. Miller, Cearcy D., and Olsen, H. Lowell: Identification of Knock in NACA High-Speed Photographs of Combustion in a Spark-Ignition Engine. NACA Rep. No. 761, 1943.

19. Miller, Cearcy D., and Logan, Walter O., Jr.: Preknock Vibrations in a Spark-Ignition Engine Cylinder as Revealed by High-Speed Photography. NACA Rep. No. 785, 1944.
20. Lindner, Werner: Mehrfachfunkenaufnahmen von Explosionsvorgängen nach der Toeplerschen Schlierenmethode. Forschungsarbeiten auf dem Gebiete des Ingenieurwesens, Heft 326, VDI-Verlag, G. m. b. H. (Berlin), 1930, S. 1–18.
21. Becker, R.: Impact Waves and Detonation. Part I. NACA TM No. 505, 1929; Part II. NACA TM No. 506, 1929.
22. Langweiler, Heinz: The Hydrodynamic Theory of Detonation. NACA TM No. 899, 1939.
23. Kast, H.: Die Brisanzbestimmung und die Messung der Detonationsgeschwindigkeit von Sprengstoffen. Zeitschr. für das Gesamte Schiess- und Sprengstoffwesen, Jahrg. 8, Nr. 8, April 15, 1913, S. 155–157.
24. Hermann, R.: Condensation Shock Waves in Supersonic Wind Tunnel Nozzles. (From Luftfahrtforschung, Bd. 19, Lfg. 6, Juni 20, 1942, S. 201–209.) R. T. P. Trans. No. 1581, Ministry of Aircraft Prod. (British).
25. Lewis, Bernard: A Chain Reaction Theory of the Rate of Explosion in Detonating Gas Mixtures. Jour. Am. Chem. Soc., vol. 52, no. 8, Aug. 1930, pp. 3120–3127.
26. Cowling, T. G.: The Influence of Diffusion of the Propagation of Shock Waves. Phil. Mag., ser. 7, vol. 33, no. 216, Jan. 1942, pp. 61–67.

U. S. GOVERNMENT PRINTING OFFICE: 1949

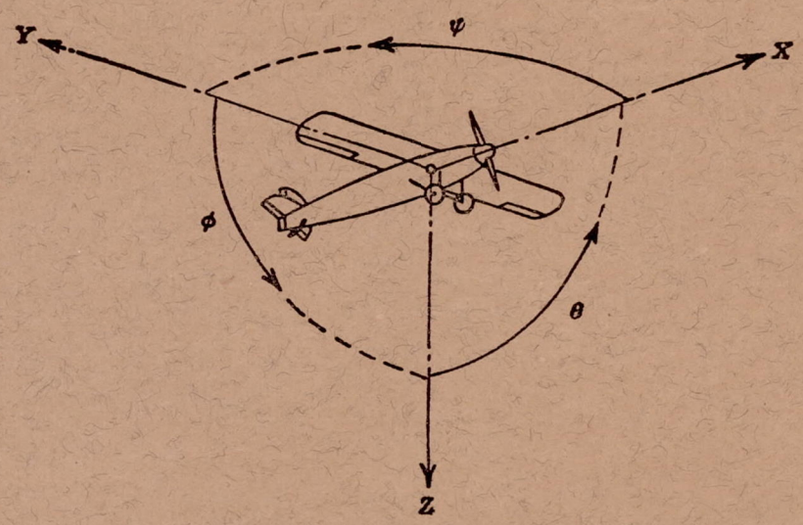


Positive directions of axes and angles (forces and moments) are shown by arrows

| Axis | | Force (parallel to axis) symbol | Moment about axis | | | Angle | | Velocities | |
|---|---|---|---|---|---|---|---|---|---|
| Designation | Symbol | | Designation | Symbol | Positive direction | Designation | Symbol | Linear (component along axis) | Angular |
| Longitudinal | $X$ | $X$ | Rolling | $L$ | $Y \longrightarrow Z$ | Roll | $\varphi$ | $u$ | $p$ |
| Lateral | $Y$ | $Y$ | Pitching | $M$ | $Z \longrightarrow X$ | Pitch | $\theta$ | $v$ | $q$ |
| Normal | $Z$ | $Z$ | Yawing | $N$ | $X \longrightarrow Y$ | Yaw | $\psi$ | $w$ | $r$ |

Absolute coefficients of moment

$C_l = \frac{L}{qbS}$ (rolling) $\quad C_m = \frac{M}{qcS}$ (pitching) $\quad C_n = \frac{N}{qbS}$ (yawing)

Angle of set of control surface (relative to neutral position), $\delta$. (Indicate surface by proper subscript.)

## 4. PROPELLER SYMBOLS

$D$ Diameter

$p$ Geometric pitch

$p/D$ Pitch ratio

$V'$ Inflow velocity

$V_s$ Slipstream velocity

$T$ Thrust, absolute coefficient $C_T = \frac{T}{\rho n^2 D^4}$

$Q$ Torque, absolute coefficient $C_Q = \frac{Q}{\rho n^2 D^5}$

$P$ Power, absolute coefficient $C_P = \frac{P}{\rho n^3 D^5}$

$C_s$ Speed-power coefficient $= \sqrt[5]{\frac{\rho V^5}{P n^2}}$

$\eta$ Efficiency

$n$ Revolutions per second, rps

$\Phi$ Effective helix angle $= \tan^{-1}\left(\frac{V}{2\pi r n}\right)$

## 5. NUMERICAL RELATIONS

1 hp=76.04 kg-m/s=550 ft-lb/sec

1 metric horsepower=0.9863 hp

1 mph=0.4470 mps

1 mps=2.2369 mph

1 lb=0.4536 kg

1 kg=2.2046 lb

1 mi=1,609.35 m=5,280 ft

1 m=3.2808 ft